# Nuclear Magnetic Resonance Studies of the Interaction between Alkali Ions and Micellar Aggregates

**Hans Gustavsson and Björn Lindman***

*Contribution from the Division of Physical Chemistry 2, The Lund Institute of Technology, Chemical Center, S-220 07 Lund 7 Sweden.* *Received November 19, 1974*

**Abstract:** $^{23}Na$ nuclear quadrupole relaxation and shielding were studied for aqueous surfactant systems in order to get information on the mode of interaction between alkali ions and aggregates of anionic amphiphiles. For aqueous solutions of sodium octanoate and sodium octyl sulfate, data can be analyzed in terms of a simple two-site model. In this way information is obtained on the association process, i.e., critical micelle concentration, premicellar aggregation, and changes in the degree of counterion association, as well as on the interactions of the micellarly bound counterions. Several derived parameters are markedly different in the two cases suggesting that the mode of counterion binding may be different for octanoate and octyl sulfate micelles. This difference is discussed and it is tentatively proposed to be due to hydrogen-bond interactions between the water of counterion hydration and carboxylate. From $^{23}Na$ relaxation times and chemical shifts, it is found that counterion binding in aqueous sodium cholate solutions changes much more gradually with concentration than in solutions of simple soaps. The continuous transition from normal to reversed micelles in the systems sodium cholate–decanol–water and sodium desoxycholate–decanol–water is found, from relaxation and chemical shift data, not to be accompanied by any marked changes in counterion binding. On the other hand, drastic changes in counterion binding take place at the highest decanol contents, probably reflecting an increasing fraction of nonassociated amphiphile. As a complement to the $^{23}Na$ NMR studies some experiments using $^{85}Rb$ and $^{133}Cs$ NMR were performed. The water isotope effect on the $^{133}Cs$ chemical shift supports conclusions drawn from $^{23}Na$ NMR studies that the alkali ions are, in general, hydrated when bound to micelles.

The self-association of amphiphilic molecules in aqueous solution to small complexes, micellar aggregates of different size and shape, and various types of liquid crystalline phases is presently the subject of intense research.[1] An elucidation of the interactions involved in the formation of aggregates of amphiphilic molecules is of considerable theoretical and technical interest and is also of great importance for the understanding of the function of many biological systems.[2] For example, the structural similarities between lamellar soap–water liquid crystals and various types of biological membranes is often emphasized.[3] In connection with the sodium–potassium pump and some other important biological processes an understanding of the interaction between alkali ions and biological membrane surfaces is of great significance.

Many experimental observations, concerned with, e.g., chemical activity,[4] translational mobility,[5] transference numbers,[6] nuclear quadrupole relaxation,[7] and nuclear shielding,[8] have shown that, in systems composed of water and an ionic amphiphile, a fraction of the counterions is more or less firmly attached to the amphiphilic aggregates. Whereas this "counterion binding" as a phenomenon is well documented, the details of the interactions involved are not well understood. Counterion binding is often considered to be an essentially nonspecific attraction of the counterions into the potential trough due to the charged amphiphilic end groups. However, several observations suggest that quite specific interactions may be involved. So, for example, micellar shape[9,10] and phase equilibria[11] may vary drastically with the counterion. Further, counterion binding to premicellar aggregates has been found to depend greatly on the surfactant end group.[12] In the present work, concerned with NMR studies of alkali ion binding to micellar aggregates, direct evidence for specific interactions between alkali ions and surfactant end groups is presented. The experimental parameters used are NMR longitudinal and transverse relaxation rates and NMR chemical shifts. While alkali ion quadrupole relaxation has been used for some years to study counterion binding in surfactant systems,[13,14] it has only recently been observed that nuclear shielding of the counterion changes at micelle formation.[8] Mainly $^{23}Na$ NMR was utilized in the present study; some complementary experiments using $^{85}Rb$ and $^{133}Cs$ NMR were also performed.

In addition to simple alkali soaps, bile salts were included in the investigation. It is now well established that these salts aggregate in aqueous systems and that they form mixed micelles with lecithin and cholesterol.[15] The biological significance of these micelles has motivated many studies aimed at an elucidation of their size and structure. Compared to simple detergents the self-association of the bile salts is very complex. Thus the formation of typical micelles is very gradual and is preceded by the formation of various small aggregates.[16-19] The alkali ion concentrations found in biological systems make it reasonable to assume that there is a significant binding of alkali ions to bile salt aggregates. This counterion binding should affect self-association equilibria and solubilization phenomena. In order to get an insight into the interaction between alkali ions and bile salt micelles, studies by NMR methods have been started. Part of the present study is concerned with the binding of sodium ions to cholate and desoxycholate micelles. The effect of solubilization of decanol was also investigated, with particular attention to the change in counterion binding occurring at the continuous transitions from normal to reversed micelles in bile salt–decanol–water systems.[20] The mixed micelles formed in the presence of cholesterol or lecithin are being studied and the results from this study will be reported separately.

## Experimental Section

Sodium octyl sulfate was bought from Merck AG and sodium octanoate from The British Drug Houses Ltd., Poole, England. These salts were used without further purification. Cholic acid was obtained from Fluka AG, Buchs, Switzerland, decanol from The British Drug Houses, and heavy water (with 99.8% isotopic enrichment) from Norsk Hydro, Norway.

Sodium cholate and sodium desoxycholate were kind gifts from Docent Krister Fontell, who also prepared several of the samples. The purity of these salts as well as their preparation have been described by Dr. Fontell previously.[16] The cesium and rubidium cholates were prepared by neutralization of cholic acid in absolute ethanol using ethanolic solutions of cesium and rubidium hydroxides,

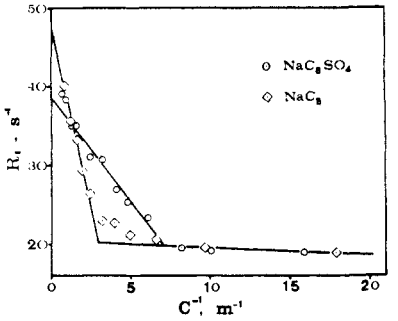


**Figure 1.** $^{23}Na$ longitudinal relaxation rates, $R_1$ ($sec^{-1}$), at 24° for aqueous solutions of sodium octyl sulfate (⊙) and sodium octanoate (◈) as a function of the inverse soap molality.

respectively. The products obtained were recrystallized twice from ethanol, and their purity was tested by nonaqueous titration with perchloric acid in acetic acid using Crystal Violet as indicator. The obtained equivalent weights were, for both salts, within 1% of the correct value.

Solutions of sodium octyl sulfate were studied freshly prepared in order to avoid hydrolysis. In the case of sodium octanoate and sodium cholate the pH of some of the solutions was determined and was found to be high enough so that no appreciable amount of the protonated salts was present. Furthermore, no dependence of $^{23}Na$ longitudinal relaxation time on pH was found in a wide range around that used in the experiments.

The spin-lattice relaxation times, $T_1$, were measured on a Bruker BK-322s spectrometer at the resonance frequency 23.81 MHz. The pulse sequence used was 180°-$t$-90° and the logarithm of the difference between the equilibrium magnetization and the magnetization following the 90° pulse was plotted as a function of time to obtain $T_1$. For the actual recording of the magnetization following the 90° pulse, a "box-car" integrator was used. Each point on the plot used to determine $T_1$ was the visual average of at least 50 separate measurements and each reported value is the average of at least three separate determinations. The accuracy of the obtained relaxation times is estimated to be about ±5%. The sample temperatures were 24 ± 2°.

A Varian V-4200 wideline NMR spectrometer equipped with a 12-in. magnet was used for the measurements of the $^{23}Na$ and $^{133}Cs$ chemical shifts and for all the line width measurements.

The $^{85}Rb$ NMR signals were recorded as the derivatives of the absorption mode signals at the resonance frequency 5.776 MHz with a modulation frequency of 20 Hz. The peak-to-peak modulation field amplitude was always less than one-fourth of the measured peak-to-peak line width. The radio-frequency field amplitude was chosen sufficiently low so that it caused a saturation broadening of less than 1%. The field inhomogeneity was found to be about 2 μT. The $^{23}Na$ line widths and the $^{23}Na$ and $^{133}Cs$ chemical shifts were recorded using the side-band technique with a modulation frequency of 400 Hz. The resonance frequency used was 15.82 MHz for sodium and 7.845 MHz for cesium, and the frequencies were stabilized within 1 Hz with crystal oscillator circuits. To improve the homogeneity and stability of the magnetic field, we employed homogeneity coils (Varian VK-3532) and a home-build superstabilizer. This gave a magnetic field inhomogeneity of about 0.7 μT. The $^{23}Na$ line widths were taken as the half-height signal widths directly from the spectra and were corrected for magnetic field inhomogeneity.

The determination of the chemical shifts was performed by the use of an external reference in a 5-mm tube coaxially inserted in the 12-mm sample tube.

The references used were a saturated aqueous solution of $NaNO_3$ for $^{23}Na$ and a 2 $m$ CsCl solution for $^{133}Cs$. These solutions have such great shifts that no distorting overlap occurs between the sample and reference signals. From the recorded spectra the shifts were measured as the distance between the centers of the reference and sample signals. These shifts were then converted into shifts relative to infinitely dilute ions in aqueous solution.

For each sample, to compensate for slight unavoidable drift in the magnetic field, the spectrum was swept up- and downfield an equal number of times. The reported values, which are averages of

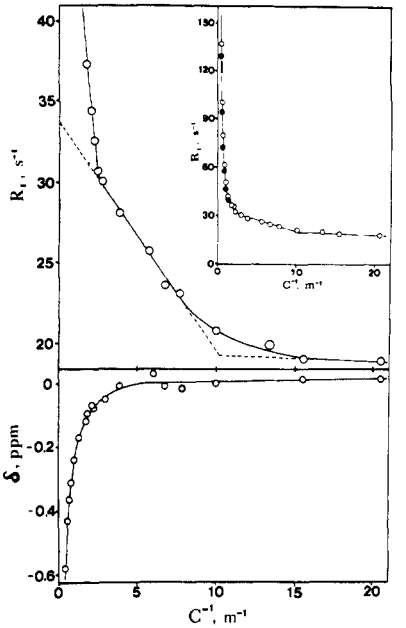


**Figure 2.** $^{23}Na$ longitudinal relaxation rates, $R_1$ ($sec^{-1}$), and $^{23}Na$ NMR chemical shifts, δ (ppm), for aqueous sodium cholate solutions, plotted as a function of the inverse cholate molality. The shifts are given relative to sodium ions at infinite dilution in water. A positive δ is a shift to higher applied field. The insert includes longitudinal relaxation rates for the high concentration region. Here also for comparison some transverse relaxation rates are given (●).

at least ten separate determinations, are estimated to have an accuracy of better than ±0.1 ppm. (For the decanol-rich solutions the precision may be slightly lower.) A positive chemical shift corresponds to a shift to higher field. In all the measurements on the wide line spectrometer the sample temperature was 26 ± 2°.

No correction of our chemical shift data for differences in macroscopic magnetic susceptibility between sample and reference solutions was made. The work by Bloor and Kidd[21] and by Templeman and van Geet[22] shows that even for extreme concentration differences between aqueous solutions the appropriate correction does not exceed our experimental error. We have found that it is only in the case of the data in Figure 5 that a significant correction should exist. Although the main features of the plots in Figure 5 are unaffected, an appropriate susceptibility correction may make the shift less dependent on decanol content at low decanol concentrations whereas the downfield shift at high decanol contents may become slightly more pronounced.

## Results

For aqueous solutions of sodium $n$-octanoate, sodium $n$-octyl sulfate, and sodium cholate the $^{23}Na$ longitudinal relaxation time ($T_1$) was studied as a function of soap concentration. The experimental data are given in Figure 1 for sodium octanoate and sodium octyl sulfate and in Figure 2 for sodium cholate. Also, for sodium cholate, line width studies giving the transverse relaxation time ($T_2$) were performed. Within experimental error $T_1$ and $T_2$ were equal at all concentrations. In order to make possible a comparison with a simple model of micelle formation (see below) the results are presented as plots of relaxation rate *vs.* the inverse surfactant concentration.

For the same systems, the chemical shift of the $^{23}Na$ NMR signal was determined. The chemical shift data are plotted as a function of inverse salt concentration in Figure 3 for sodium octanoate and sodium octyl sulfate and in Figure 2 for sodium cholate. The shifts, δ, are given relative to an infinitely dilute aqueous solution of sodium ion.

A positive chemical shift denotes a shift to higher applied field. The shifts were obtained with a saturated sodium nitrate solution as reference, but were converted to the shift

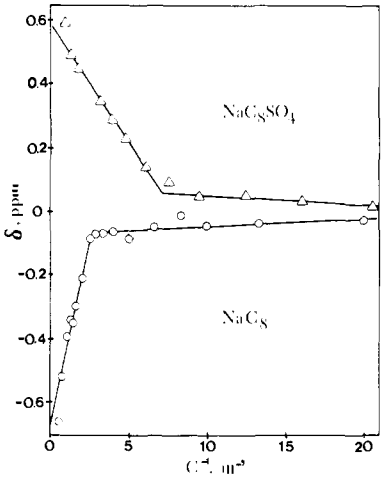


**Figure 3.** $^{23}Na$ NMR chemical shifts, $\delta$ (ppm), at 26° for aqueous solutions of sodium octyl sulfate (△) and sodium octanoate (○), as a function of the inverse soap molality. The shifts are given relative to sodium ions at infinite dilution in water. A positive shift is to higher applied field.

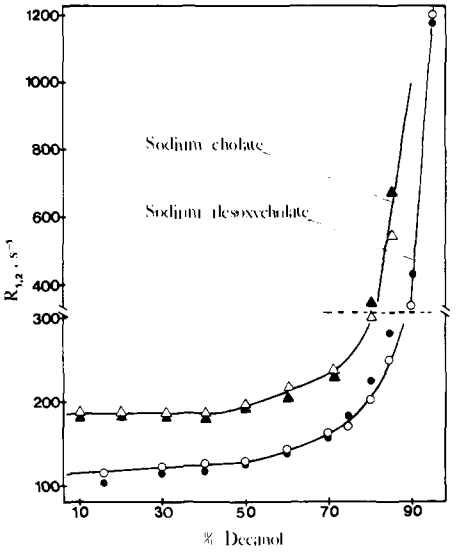


**Figure 4.** $^{23}Na$ longitudinal, $R_1$ ($sec^{-1}$), and transverse, $R_2$ ($sec^{-1}$), relaxation rates for solutions containing sodium cholate (△ and ▲) or desoxycholate (○ and ●), decanol, and water as a function of the weight percentage of decanol. The salt to water weight ratios were kept constant at 1.22 and 1.00 for cholate and desoxycholate, respectively. Filled symbols give $R_2$ values and open symbols $R_1$ values.

scale mentioned, from studies of the shift between the saturated sodium nitrate solution and solutions with different concentrations of sodium chloride.

The phase diagrams[20] of the three-component systems sodium cholate–decanol–water and sodium desoxycholate–decanol–water show as an interesting feature, an amorphous liquid isotropic phase extending all the way from the water corner to the decanol corner. It has been shown[20] that the solutions are molecule-disperse at the higher water and decanol concentrations, respectively. However, in the rest of the phase region, various types of aggregates exist with a continuous transition from a region with normal micelles to one with micelles of the reversed type. In order to elucidate the changes in counterion binding accompanying the changes in aggregation, $^{23}Na$ NMR studies were performed. In Figure 4 $^{23}Na$ relaxation rates are given as a function of weight percentage of decanol at a constant ratio of salt to water for the two systems mentioned. Both the

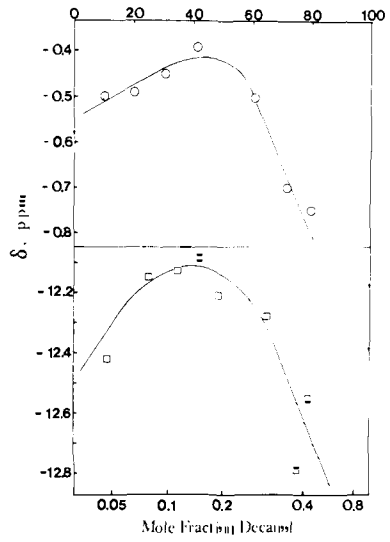


**Figure 5.** $^{23}Na$ (○) and $^{133}Cs$ (□) NMR chemical shifts, $\delta$ (ppm), at 26° for solutions composed of sodium or cesium cholate, decanol, and water plotted against the decanol concentration. The molar ratios of cholate to water were kept constant at 0.0511 in both cases. (This is the same molar ratio as used for the $^{23}Na$ relaxation studies represented in Figure 4.) The weight-percentage scale is valid for the case of sodium cholate whereas the mole fraction scale applies to both systems.

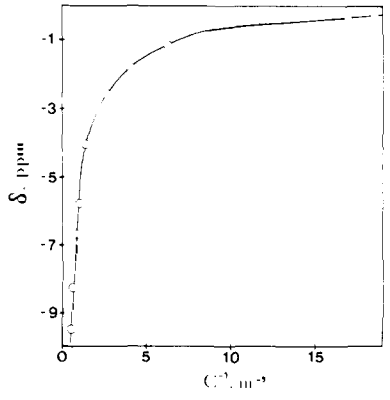


**Figure 6.** $^{133}Cs$ NMR chemical shifts, $\delta$ (ppm), at 26° for aqueous cesium cholate solutions as a function of the inverse cholate molality. The shifts are given relative to cesium ions at infinite dilution in water. Shifts to higher field are positive.

longitudinal ($R_1$) and the transverse ($R_2$) relaxation rates are given. $R_2$ was obtained from the line width of the absorption NMR signal with a correction for the magnetic field inhomogeneity. In the case of slow relaxation, $R_1$ is more reliable than $R_2$ because of the effect of magnetic field inhomogeneity, whereas the reverse is true in the case of very rapid relaxation. $^{23}Na$ chemical shift data for the system sodium cholate–decanol–water are given in Figure 5 as a function of the decanol concentration.

As a complement to the $^{23}Na$ studies, limited $^{85}Rb$ and $^{133}Cs$ NMR studies were performed. For $^{85}Rb$ the transverse relaxation rate was determined from the line width of the absorption mode derivative spectra whereas for $^{133}Cs$ chemical shift measurements were performed. $^{85}Rb$ relaxation rates obtained for the rubidium cholate–decanol–water system are given in Table I and some experiments with octyl sulfate solutions are described below. The concentration dependence of the $^{133}Cs$ chemical shift of aqueous cesium cholate solutions is presented in Figure 6. In Figure 5 $^{133}Cs$ chemical shifts are given as a function of the decanol concentration for the system cesium cholate–decanol–water.

Table I. $^{85}Rb$ and $^{23}Na$ Relaxation Rates, $R_{obsd}$, and Ratios $R_{obsd}/R_0$[a] for Some Rubidium Cholate and Sodium Cholate Solutions

| Sample composition, mol % | | | $Rb^+$ | | $Na^+$ | |
|---|---|---|---|---|---|---|
| Cholate | Water | Decanol | Relaxation rate, $R_{2,obsd}$ ($sec^{-1}$) | Ratio $R_{2,obsd}/R_{2,0}$ | Relaxation rate, $R_{1,obsd}$ ($sec^{-1}$) | Ratio $R_{1,obsd}/R_{1,0}$ |
| 0.74 | 99.26 | 0 | 895 | 1.95 | 30.7 | 1.66 |
| 1.15 | 98.85 | 0 | 980 | 2.13 | 42.0 | 2.27 |
| 2.67 | 97.33 | 0 | 1,965 | 4.27 | 80.1 | 4.32 |
| 4.19 | 82.03 | 13.78 | 6,590 | 14.3 | 187 | 10.1 |
| 2.56 | 48.56 | 48.98 | 11,600 | 25.1 | 300 | 16.2 |

[a] The $R_0$'s are relaxation rates of rubidium and sodium ions in dilute aqueous solutions. The values used are $R_{2,0} = 460$ $sec^{-1}$ and $R_{1,0} = 18.5$ $sec^{-1}$ for $Rb^+$ and $Na^+$, respectively.

Table II. Effect of Substitution of $D_2O$ for $H_2O$ on $^{23}Na$ Longitudinal Relaxation Rate, $R_1$, for Samples Composed of Sodium Cholate, Decanol, and Water

| Sample composition, mol % | | | Relaxation rates, $R_1$ ($sec^{-1}$) | | |
|---|---|---|---|---|---|
| Sodium cholate | Decanol | $H_2O$ or $D_2O$ | With $D_2O$ | With $H_2O$ | Ratio[a] $R_{1,D_2O}/R_{1,H_2O}$ |
| 3.3 | 0 | 96.7 | 133 | 110 | 1.24 ± 0.03 |
| 4.2 | 13.6 | 82.0 | 248 | 214 | 1.22 ± 0.03 |
| 2.5 | 49.0 | 48.5 | 319 | 282 | 1.22 ± 0.03 |

[a] Obtained after a correction described in the text.

The water isotope effect was studied with $^{23}Na$ in the case of relaxation rates and with $^{133}Cs$ in the case of chemical shifts. The ratio of the longitudinal relaxation rate for solutions containing $D_2O$ to those containing $H_2O$ was found to be 1.22–1.24 for three samples in different parts of the sodium cholate–decanol–water system (Table II). In obtaining these values, a linear correction was applied for the dilution of $D_2O$, which arose from the deuteron exchange with decanol and cholate hydroxyls.

It has been noted in previous work[23,24] that for the halide ions and at least the heavier ions, exchange of $D_2O$ for $H_2O$ in aqueous alkali halide solution markedly changes the nuclear shielding. In order to examine if this effect prevails also in micellar solutions, the $^{133}Cs$ chemical shifts of aqueous solutions of cesium *n*-dodecanoate were measured. It was found that even at high concentrations no significant reduction of the water isotope effect below the value observed for cesium chloride solutions occurs. So, for example, for a 1.5 *M* cesium dodecanoate solution the chemical shift was found to be 0.85 ppm higher with $D_2O$ as solvent than with $H_2O$. Similar observations have been made with aqueous solutions of *n*-dodecyltrimethylammonium chloride using $^{35}Cl$ NMR.[25]

## Discussion

**Relaxation.** The relaxation of both $^{23}Na$ and $^{85}Rb$ nuclei in solution is generally dominated by time-modulated interactions between the nuclear electric quadrupole moments and electric field gradients at the nuclei. Previous studies[7,20,26-28] provide the basis for a general interpretation of the quadrupole relaxation of counterions in surfactant systems. It may be demonstrated[7,10,27] by studying the frequency dependence of the relaxation time or by comparing the longitudinal ($T_1$) and transverse ($T_2$) relaxation times that extreme narrowing conditions normally apply. As can be seen from Figures 2 and 4 the equality of $T_1$ and $T_2$ is demonstrated to hold, within the experimental error, over a wide range of relaxation rates for some of the systems considered in this treatment. Under conditions of extreme narrowing the relaxation rates may be written[29]

$$\frac{1}{T_1} = \frac{1}{T_2} = \frac{3}{40}\left(\frac{e^2qQ}{\hbar}\right)^2 \frac{2I+3}{I^2(2I-1)}\tau_c \qquad (1)$$

Here $I$ is the spin quantum number which is $\frac{3}{2}$ for $^{23}Na$ and $\frac{5}{2}$ for $^{85}Rb$, $eQ$ the nuclear electric quadrupole moment, and $eq$ the largest component of the electric field gradient tensor being modulated by the molecular motion. (The gradient, assumed to have cylindrical symmetry, is taken in its principal axes system.) $\tau_c$ is the time constant of the variation of the field gradient. In those cases where line width was measured, $T_2$ was obtained either from $T_2^{-1} = \pi\Delta\nu_{1/2}$ or from $T_2^{-1} = \pi\sqrt{3}\Delta\nu_{pp}$, where $\Delta\nu_{1/2}$ is the line width at half-height of the absorption peak and $\Delta\nu_{pp}$ the peak-to-peak line width of the absorption mode derivative signal.

In cases where the nuclei studied undergo rapid (compared to relaxation) exchange between different sites having different relaxation rates, the resulting longitudinal or transverse relaxation rates are given by

$$R_{obsd} = \sum_i p_i R_i \qquad (2)$$

where $p_i$ is the fraction of nuclei in site $i$ and $R_i$ is the intrinsic longitudinal or transverse relaxation rate of site $i$. Previous studies[7,10,14,27] of the temperature dependence of the relaxation rate and of the counterion isotope effect have demonstrated that counterion exchange is rapid compared to relaxation and that eq 2 can be assumed to apply for the systems studied here.

It will be assumed that for counterions in micellar solutions only two binding sites have to be considered; i.e., the counterions are either free or attached to the micelles. Further we assume as a first approximation that the ratio of counterions to surfactant ions in the micelles is independent of concentration and that the pseudo-phase separation model of micelle formation applies. It may be shown,[7,27] that, with these assumptions, for concentrations below the critical micelle concentration (cmc) one obtains the relation

$$R_{obsd} = R_f \qquad (3a)$$

which should be approximately independent of soap concentration. Above the cmc

$$R_{obsd} = R_f + \beta(R_m - R_f) - \frac{\beta \cdot cmc}{C_t}(R_m - R_f) \qquad (3b)$$

Here $R_f$ and $R_m$ are the intrinsic relaxation rates of free and micellarly bound counterions, respectively, $\beta$ is the ratio of counterions to surfactant ions in the micelles, and $C_t$ is the total surfactant concentration.

According to eq 3 we expect, for the simple model considered, to obtain two straight lines intersecting at the critical micelle concentration if the relaxation rate is plotted against the inverse soap concentration. As can be inferred from Figure 1, $R_{1,obsd}$ of $^{23}Na$ for sodium octanoate and sodium octyl sulfate solutions follows the predicted behavior over a wide concentration range around the cmc. From the intersection points of the two straight lines the cmc's are obtained as 0.37 *m* for sodium octanoate and as 0.14 *m* for sodium octyl sulfate. These values are in good agreement with

cmc determinations by means of other methods.[5,30] In the case of sodium octanoate there appears to be a marked increase in $R_1$ at concentrations considerably below the cmc. The increase in $R_1$ appears to start in the concentration region where the onset of formation of smaller complexes has been inferred from other experimental quantities (see ref 5 and literature cited therein). No corresponding increase is observed in the case of sodium octyl sulfate. This indication that sodium ions bind to premicellar complexes in the case of octanoate but not in the case of octyl sulfate is in agreement with recent observations[12] of differences in counterion binding to premicellar aggregates between surfactants with different end groups. It should be noted, however, that an inapplicability of the pseudo-phase separation model may give rise to some curvature in the plots around the cmc. Deviations from the behavior predicted, corresponding to an enforced quadrupole interaction, occur also in the high concentration region (which was not studied in detail), i.e., above about 1.2 *m* for sodium octanoate and 0.8 *m* for sodium octyl sulfate. These slope alterations in the plots may be due to increases in $\beta$ and/or $R_m$. For sodium octanoate the enhanced relaxation starts at about the same concentration as that at which self-diffusion data have demonstrated an increase in the ratio of counterions to surfactant ions in the micelles.[5]

From the slopes or intercepts of the straight lines above the cmc in Figure 1, $\beta(R_m - R_f)$ is obtained (using $R_f$ values extrapolated to the cmc) as 28 $sec^{-1}$ for sodium octanoate and as 20 $sec^{-1}$ for sodium octyl sulfate. If we assume $\beta = 0.6$ (cf. ref 5 and references therein) we get $R_m = 66$ $sec^{-1}$ for sodium octanoate and $R_m = 52$ $sec^{-1}$ for sodium octyl sulfate. For the ratio of $R_m$ to $R_0$, the $^{23}Na$ relaxation rate at infinite dilution in water, we obtain 3.48 and 2.77 for sodium octanoate and sodium octyl sulfate, respectively. ($R_m/R_0$ is given by $q_m^2\tau_{cm}/q_0^2\tau_{c0}$ where the subscripts on $q$ and $\tau_c$ are as above.)

$^{85}Rb$ transverse relaxation rates for aqueous rubidium octanoate solutions are given in ref 7 and using the same procedure as above we obtain $R_m/R_0 = 3.46$.

In order to obtain information on the relative binding affinities of alkali ions to octyl sulfate micelles and to obtain an estimate of $R_m/R_0$ for $^{85}Rb^+$ the following experiments were performed. For a 0.5 *M* sodium octyl sulfate solution the effect on the $^{23}Na$ longitudinal relaxation of adding LiCl, NaCl, or RbCl (to a final concentration of 0.5 *M*) was investigated. $T_1$ was found to increase from 29.3 msec to 31.0, 33.0, and 35.5 msec on addition of LiCl, NaCl, and RbCl, respectively. If these differences can be referred solely to competitive binding of the different alkali ions it is clear that according to eq 2 (cf. also ref 31) the affinities of binding to the micelles are in the sequence $Rb^+ > Na^+ > Li^+$. For the solution containing 0.5 *M* sodium octyl sulfate and 0.5 *M* RbCl the $^{85}Rb$ transverse relaxation rate was determined to be 1580 $sec^{-1}$, and we obtained for this solution $R_{obsd}/R_0 = 1.9$ for $^{23}Na$ and $R_{obsd}/R_0 = 3.5$ for $^{85}Rb$. This indicates that in the case of octyl sulfate micelles $R_m/R_0$ is considerably greater for $Rb^+$ than for $Na^+$. $R_m/R_0$ for $Rb^+$ bound to octyl sulfate micelles was estimated as 7.0 assuming that the total concentration of bound counterions is the same for the solution containing sodium octyl sulfate and NaCl as for that containing sodium octyl sulfate and RbCl. Although this value of $R_m/R_0$ is approximate there is no doubt that $R_m/R_0$ is greater for $Rb^+$ bound to octyl sulfate micelles than for $Rb^+$ bound to octanoate micelles.

In order to understand the relaxation rates of the micellarly bound counterions we must identify the motion causing relaxation. From a recent investigation[28] of this problem it appears that the absence of changes in relaxation rate at phase transitions,[32] as well as some other observations, strongly indicates that a local motion, and not a motion over the micellar dimensions, is causing relaxation. For a number of cases the relaxation rate has been found to increase by ca. 20% on substitution of $D_2O$ for $H_2O$. This is the same change as observed for nonassociated hydrated ions[33] and corresponds to the isotope effect in water viscosity and water translational diffusion.[34] It is reasonable to assume then that the motion causing relaxation is somehow connected with the motion of the water molecules. The alkali ions in micellar solutions can be assumed to be hydrated (cf. ref 13 and the chemical shift data presented above). One motional process which may give a rationalization of counterion relaxation data in surfactant systems is the exchange of the hydrated counterion between the micellar surface and the intermicellar solution.[28]

The difference in behavior of $R_m/R_0$ between octanoate and octyl sulfate micelles indicates that there may be a marked difference in the mode of interaction between counterion and surfactant end group in the two cases. Mukerjee[35] has proposed that, for carboxylate end groups, hydrogen bonding between the surfactant end group and the water of counterion hydration should be important, whereas this mechanism should not be significant for alkyl sulfates with their low basicities. For octyl sulfate micelles then, simple electrostatic interactions should explain counterion binding and we expect affinities to increase with decreasing radius of the hydrated alkali ion. Furthermore, since in the relaxation mechanism considered above the field gradients decrease rapidly with increasing distance between bound counterion and surfactant end group,[28] we expect a considerably greater relative change in the field gradient on binding to the micelles of the more weakly hydrated $Rb^+$ ion than with $Na^+$. Thus we expect $R_m/R_0$ to be considerably greater for $Rb^+$ than for $Na^+$ for nonspecific electrostatic binding. It appears that our results on relative affinities, as well as on the relaxation rates, are in agreement with the predicted behavior for octyl sulfate micelles.

The observations that, for octanoate micelles $R_m/R_0$ has approximately the same value for $Rb^+$ and $Na^+$ and that $R_m$ is greater for $Na^+$ bound to octanoate micelles than when it is bound to octyl sulfate micelles, are consistent with the proposal that, in addition to electrostatic effects, hydrogen bonding effects are significant in the case of octanoate micelles. Hydrogen bonding should be more effective in the case of the more strongly polarizing sodium ion. Since the motion causing relaxation involves the motion of the water molecules, the greater $R_m$, in the case of octanoate micelles for $Na^+$, is in line with a reduced mobility of the water molecules as a result of hydrogen bonding to the soap end group.

The model proposed above for the relaxation process and for the interactions involved in the counterion binding to micelles appears to get further support from the data presented recently by Robb and Smith.[36] A further demonstration of the difference in interaction mechanism between the two cases is provided by the chemical shift data which will be discussed below.

From the $^{23}Na$ longitudinal and transverse relaxation rates presented in Figure 2, it is apparent that cholate micelles behave quite differently from the simple soap micelles considered so far. The fact that, for sodium cholate solutions, changes in counterion relaxation rate are more gradual, implies that the aggregation process is more complex involving complexes of different size and structure. If the plot in Figure 2 is analyzed in terms of the simple model considered above, we obtain for the cmc 0.10 *m* and, furthermore, there appears to be a marked change in counterion binding at ca. 0.41 *m*. The cmc value obtained agrees

closely with the concentration at which aggregates of micellar dimensions appear to form according to investigations using other methods.[16-19] The enhanced counterion binding observed at 0.41 *m* strongly indicates a change in the micellar structure, which is also proposed in studies using other experimental techniques.[16-19]

For the aggregates which start to form at about 0.1 *m* the quantity $\beta(R_m - R_f)$ is obtained as above to be 15 $sec^{-1}$ for the cholate micelles. The fact that this value is markedly lower than that for octanoate micelles, where the same polar end groups occur, can probably be referred to a considerably lower degree of counterion association. This is expected since bile salt micelles, as a result of the detergent molecular structure, should have considerably larger areas per carboxylate group than normal detergent micelles. Making the unexamined assumption that $R_m$ is the same in the two cases we obtain for cholate $\beta$ = ca. 0.3.

Fontell[20] has demonstrated that in the three-component systems sodium cholate–decanol–water and sodium desoxycholate–decanol–water there is a continuous transition from normal to reversed micelles. The transition appears to occur at a decanol concentration of about 50% by weight, whereas above about 90% by weight of decanol, micelles do not form.[20] As can be seen in Figure 4 the $^{23}Na$ transverse and longitudinal relaxation rates are, except for the highest decanol contents, only moderately dependent on decanol concentration. These results have some interesting implications concerning the counterion binding and the relaxation mechanism. First, while small slope alterations in Figure 4 may be present in the range 45–50% decanol by weight, there appear to be no major changes in counterion binding at the transition from normal to reversed micelles. On the other hand, drastic changes take place at the transition from reversed micellar to molecule-disperse decanolic solutions. This is explainable in terms of a model with hydrated counterions in the water cores of the reversed micelles. As long as the reversed micelles exist, the sodium ions can retain binding and hydration properties similar to those in solutions containing normal micelles, but as the reversed micelles break down the counterions probably become partially dehydrated and therefore interact more strongly with the amphiphilic anions forming some type of ion pairs. This picture explains the weak dependence of relaxation rate on decanol concentration in the micellar region and an extensive hydration of the sodium ions is also implied by the experiments concerned with the water isotope effect (Table II).

Also for an understanding of the relaxation mechanism the data presented in Figure 4 are significant. The observation that the relaxation rate remains nearly unchanged, even on drastic changes in aggregate curvature and size as well as in viscosity,[20] tends to exclude a motion over the dimensions of the aggregates (micellar rotation and lateral diffusion of counterions or amphiphile) as a possible relaxation mechanism. Instead a local motion, for which some other arguments are given in ref 28, is strongly proposed as the cause of relaxation. The observed water isotope effect suggests this local motion to involve the displacement of water molecules. The transverse and longitudinal relaxation times are the same, within experimental error, even at very high decanol contents, implying that the correlation time is always considerably less than $10^{-8}$ sec.

The $^{85}Rb$ relaxation rates given in Table I show a behavior similar to the $^{23}Na$ relaxation rates. A comparison between $^{85}Rb$ and $^{23}Na$ of the relative relaxation rates, $R_{obsd}/R_0$, is also made in Table I. In decanol-free solutions $R_{obsd}/R_0$ is approximately the same for the two counterions and since this was also found for octanoate micelles the mode of counterion binding is proposedly the same in these two cases. As decanol is added $R_{obsd}/R_0$ of $Rb^+$ becomes considerably greater than that of $Na^+$. This can probably be referred to differences in hydration properties between the two ions. Thus the more strongly hydrated sodium ion is expected to be influenced to a quite small extent by environmental changes, whereas, for $Rb^+$, decanol addition may cause a partial dehydration.

**Shielding.** As a complement to our quadrupole relaxation studies, investigations on the same systems of the counterion chemical shifts were performed. It was recently discovered that the counterion nuclear shielding starts to change at the critical micelle concentration[8] and that the method, therefore, should be useful in exploring ion interactions in amphiphilic systems. In comparison to the quadrupole relaxation rates, which depend also on microdynamic properties, the chemical shifts should contain information more directly related to the mode of interaction. However, whereas the theory of quadrupole relaxation is quite well developed, understanding of the chemical shifts of alkali and halide ions is, even for simple solutions, very incomplete. From an experimental point of view, however, the dependence of, especially the $^{23}Na$ chemical shifts, on environmental changes has been fairly extensively studied. Bloor and Kidd[37] showed from theoretical estimates that, for sodium ions in solution, the shift is dominated by paramagnetic effects. Therefore, it is reasonable to interpret $^{23}Na$ chemical shifts in terms of an overlap of the outer p orbitals of the sodium ion with the outer s and p orbitals of surrounding solvent molecules or ions. This interpretation advanced by Bloor and Kidd was supported by their own investigations on the solvent dependence of the shielding.[37] Also the more extensive studies on the solvent effect presented by Popov et al.[38-40] showed a very good correlation between $^{23}Na$ chemical shift and solvent electron donor ability. Alkali ion chemical shifts in the presence of other ions have been studied for a number of aqueous solutions.[21,22,41,42] The effect of a large number of anions on the chemical shift of the alkali ions in water was found to be explainable in a way analogous to the solvent effect, i.e., that the more strongly electron-donating is the anion the greater is the downfield shift observed.[21,22] Since a considerable paramagnetic contribution to the shift is due to the water molecules it is important to take into account also the modification of this term arising from the presence of other species in the solution.

Although a quantitative interpretation of our $^{23}Na$ and $^{133}Cs$ chemical shift data is impossible, the studies cited above provide us with a good basis for qualitative considerations.

The concentration dependence of the chemical shift can be rationalized using the same model as used above for the quadrupole relaxation rate. Thus assuming a two-site model with a constant counterion association degree and the applicability of the pseudo-phase separation model of micelle formation, we obtain, using the same notation as above, for concentrations below the cmc

$$\delta_{obsd} = \delta_f \quad (4a)$$

and for concentrations above the cmc

$$\delta_{obsd} = \delta_f + \beta(\delta_m - \delta_f) - \frac{\beta \cdot cmc}{C_t}(\delta_m - \delta_f) \quad (4b)$$

It can be seen from Figure 3 that the data obtained for solutions of sodium octanoate and sodium octyl sulfate conform closely to the simple model considered. From the intersection points of the straight-line segments in Figure 3, we obtain for the cmc the values 0.38 and 0.14 *m* for sodium octanoate and sodium octyl sulfate, respectively. These values are in good agreement with those obtained from the $^{23}Na$ relaxation rates and with the literature values cited above.

Deviations from the simple model occur at higher concentrations (about 1.2 *m* for octanoate and 0.8 *m* for octyl sulfate) and indicate an enforced counterion binding characterized by increases in either $\beta$ or $|\delta_m - \delta_f|$ or both. The qualitative binding information derived is again in agreement with that derived from quadrupole relaxation rates and translational mobilities.[5]

From the slopes or intercepts of the plots in Figure 3 the quantity $\beta(\delta_m - \delta_f)$ is obtained as −0.56 ppm for octanoate micelles and as 0.53 ppm for octyl sulfate micelles. The fact that the chemical shift changes in opposite direction on micelle formation in the two cases deserves special consideration. According to the general discussion of alkali ion chemical shifts which was given above, these observations imply (relative to the "free" hydrated sodium ion) an enforced overlap between the outer sodium orbitals and the orbitals of surrounding species in the case of octanoate micelles. In contrast, this overlap should be reduced in the case of octyl sulfate micelles.

The discussion of the relaxation data led to the conclusion that the alkali ions are hydrated when bound to the micelles, and further support for this idea is provided by the results given above concerning the water isotope effect in the $^{133}Cs$ chemical shift. Thus we find, within our experimental error, the same difference in chemical shift between $D_2O$ and $H_2O$ solutions for micellar cesium dodecanoate solutions as for cesium chloride solutions. (We believe that the water isotope effect in alkali and halide ion chemical shifts is in general a most interesting way of probing into the hydration properties of small ions and further studies on a variety of amphiphilic systems are in progress.)

If we make the reasonable assumption that the sodium ions are hydrated at the micellar surface, then what we observe are modifications of the sodium–water overlap. Consequently, the water of sodium ion hydration has a greater electron donating ability when the sodium ion is bound to an octanoate micelle than when it is free in the bulk solution. For the case of octyl sulfate micelles the reverse situation should apply. This difference between the two cases should have a significant bearing on the understanding of the mechanism of counterion binding. While detailed conclusions, in view of the deficient theoretical understanding of alkali ion chemical shifts, are somewhat dangerous, the fact must be pointed out that our observations appear to offer good support for the proposal[35] that hydrogen-bond interactions between surfactant end group and water of counterion hydration are of great importance.

Thus we may explain the observation that the paramagnetic shielding is markedly greater in the case of octanoate micelles than in the case of octyl sulfate micelles in the following way. In the case of octanoate, hydrogen bonds between $-CO_2^-$ and water are significant. For a water molecule belonging to the hydration sheath of a sodium ion, hydrogen bonding will be strengthened as a result of the great polarizing ability of the sodium ion. As a consequence of the hydrogen bonding, the water oxygens acquire greater negative charge and thus become more strongly electron donating. In view of the low basicity of the sulfate end group the mechanism postulated for octanoate should not be appreciable for the octyl sulfate micelles. Although alternative interpretations of our data are possible, the consistent picture provided by chemical shift and relaxation data should make it important to further investigate, by other independent methods, the model considered here.

The $^{23}Na$ and $^{133}Cs$ chemical shift data for cholate solutions (given in Figures 3 and 6) show, in comparison with the simple surfactants, a more gradual change in counterion chemical shift with concentration. The quantity $\delta_m - \delta_f$ obviously has the same sign for cholate micelles as in the case of octanoate micelles, pointing to a similar interaction in the two cases, but, in view of the gradual change in counterion binding with concentration, a determination of the shift of micellarly bound counterions is impossible for the cholate solutions.

Studies of the $^{23}Na$ and $^{133}Cs$ chemical shifts of solutions containing sodium or cesium cholate, decanol, and water show relatively small variations in $\delta$ with decanol content as long as it is 70% or lower. However, above this value, a marked downfield shift is observed (Figure 5). This is consistent with what was inferred from the counterion quadrupole relaxation rates above; i.e., the changes in counterion binding are small at the transition from normal to reversed micelles but that marked changes occur when the decanol content approaches values where the reversed micelles cease to exist. The great downfield shift observed at high decanol contents can probably be referred to an enforced interaction between the hydrated counterion and the charged amphiphile end group.

The data presented in Figure 5 also give significant information on counterion hydration. Thus, according to the study of Erlich and Popov,[38] the complete exchange of alcohol molecules for the hydration sheath of $Na^+$ is expected to lead to an upfield shift of several parts per million. Such a tendency is not observed and, therefore, further support is provided for our conclusion that the counterions remain extensively hydrated at quite low water concentrations.

**Acknowledgments.** We are most grateful to Dr. Krister Fontell for his generous experimental advice and assistance as well as for discussions and to Mr. Jan Andrasko and Dr. Tom Bull for their help with the relaxation time measurements. We are indebted to Dr. Håkan Wennerström for helpful discussions on relaxation theory. B. L. is grateful to Professor Pasupati Mukerjee for an invitation to visit his laboratory and for valuable discussions. Mr. Dennis Burton kindly made a linguistic revision of the manuscript.

## References and Notes

(1) P. Ekwall and P. Stenius, *Phys. Chem., Ser. 2*, in press.
(2) C. Tanford, "The Hydrophobic Effect. Formation of Micelles and Biological Membranes", Wiley, New York, N.Y., 1973.
(3) G. Szabo in "Membrane Molecular Biology", C. F. Fox and A. Keith, Ed., Sinauer Associates, Stamford, Conn., 1972, p 146.
(4) W. K. Mathews, J. W. Larsen, and M. J. Pikal, *Tetrahedron Lett.*, **6**, 513 (1972).
(5) B. Lindman and B. Brun, *J. Colloid Interface Sci.*, **42**, 388 (1973).
(6) C. W. Davies, "Ion Association", Butterworths, London, 1962, p 117.
(7) B. Lindman and I. Danielsson, *J. Colloid Interface Sci.*, **39**, 349 (1972).
(8) H. Gustavsson and B. Lindman, *J. Chem. Soc., Chem. Commun.*, 93 (1973).
(9) F. Reiss-Husson and V. Luzzati, *J. Phys. Chem.*, **68**, 3504 (1964).
(10) G. Lindblom, B. Lindman, and L. Mandell, *J. Colloid Interface Sci.*, **42**, 400 (1973).
(11) P. Ekwall, *Adv. Liquid Cryst.*, in press.
(12) B. Lindman, N. Kamenka and B. Brun, *C. R. Acad. Sci., Ser. C*, **278**, 393 (1974).
(13) B. Lindman and P. Ekwall, *Mol. Cryst.*, **5**, 79 (1968).
(14) B. Lindman and P. Ekwall, *Kolloid Z. Z. Polym.*, **234**, 1115 (1969).
(15) D. M. Small in "The Bile Acids", Vol. 1, P. P. Nair and D. Kritchevsky, Ed., Plenum Press, New York, N.Y., 1971, p. 249.
(16) K. Fontell, *Kolloid Z. Z. Polym.*, **244**, 246 (1971).
(17) K. Fontell, *Kolloid Z. Z. Polym.*, **244**, 253 (1971).
(18) K. Fontell, *Kolloid Z. Z. Polym.*, **246**, 614 (1971).
(19) K. Fontell, *Kolloid Z. Z. Polym.*, **246**, 710 (1971).
(20) K. Fontell, *Kolloid Z. Z. Polym.*, **250**, 825 (1972).
(21) E. G. Bloor and R. G. Kidd, *Can. J. Chem.*, **50**, 3926 (1972).
(22) G. J. Templeman and A. L. van Geet, *J. Am. Chem. Soc.*, **94**, 5578 (1972).
(23) A. Lowenstein, M. Shporer, P. C. Lauterbur, and J. E. Ramirez, *Chem. Commun.*, 214 (1968).
(24) J. Blaser, O. Lutz, and W. Steinkilberg, *Z. Naturforsch., Teil A*, **27**, 72 (1972).
(25) H. Gustavsson and B. Lindman, to be submitted for publication.
(26) I. D. Robb, *J. Colloid Interface Sci.*, **37**, 521 (1971).
(27) G. Lindblom and B. Lindman, *J. Phys. Chem.*, **77**, 2531 (1973).
(28) H. Wennerström, G. Lindblom, and B. Lindman, *Chem. Scr.*, **6**, 97 (1974).
(29) A. Abragam, "The Principles of Nuclear Magnetism", Clarendon Press, Oxford, 1961, p 314.
(30) P. Mukerjee and K. J. Mysels, *Nat. Stand. Ref. Data. Ser., Nat. Bur.*

*Stand.*, **No. 36** (1971).
(31) B. Lindman and I. Lindqvist, *Chem. Scr.*, **1**, 195 (1971).
(32) G. Lindblom and B. Lindman in "Chemie, Physikalische Chemie und Anwendungstechnik der grenzflächenaktiven Stoffe", Vol. II, Carl Hanser Verlag, München, 1973, p 925.
(33) M. Eisenstadt and H. L. Friedman, *J. Chem. Phys.*, **44**, 1407 (1966).
(34) G. S. Kelly in "Water, a Comprehensive Treatise", Vol. 1, F. Franks, Ed., Plenum Press, New York, N.Y., 1972, p 363.
(35) P. Mukerjee, personal communication.
(36) I. D. Robb and R. Smith, *J. Chem. Soc., Faraday Trans. 1*, **70**, 287 (1974).
(37) E. G. Bloor and R. G. Kidd, *Can. J. Chem.*, **46**, 3425 (1968).
(38) R. H. Erlich and A. L. Popov, *J. Am. Chem. Soc.*, **93**, 5620 (1971).
(39) M. Herlem and A. I. Popov, *J. Am. Chem. Soc.*, **94**, 1431 (1972).
(40) M. S. Greenberg, R. L. Bodner, and A. I. Popov, *J. Phys. Chem.*, **77**, 2449 (1973).
(41) C. Deverell and R. E. Richards, *Mol. Phys.*, **10**, 551 (1966).
(42) O. Lutz, *Z. Naturforsch., Teil A*, **23**, 1202 (1968).

# Bond Length Variations in Substituted Phosphoranes

**James M. Howell**

*Contribution from the Department of Chemistry, Brooklyn College, City University of New York, Brooklyn, New York 11210.* *Received November 11, 1974*

**Abstract:** Successive methylation or hydrogenation in the equatorial position of fluorophosphoranes produces strong decreases in the (P-F) axial overlap population obtained from extended Hückel calculations in agreement with experimental data. The trends are rationalized in terms of a repulsive interaction between the lone pairs of the axial fluorine atoms and the equatorial $\sigma$ bonds. The structures of $PF_5$, $PF_4CH_3$, and $PF_3(CH_3)_2$ were optimized by the CNDO/2 method confirming the overlap population trends.

There has been a recent flush of interest in the molecular orbitals of phosphoranes at both the semiempirical[1] and ab initio levels.[2-5] Most of these studies have been directed at d orbital participation,[1,4] the pseudo-rotational process,[1-3] or conformational effects.[1,3,5] In this paper we examine another facet of phosphorane chemistry, bond length variation with substituent. It has been known[6] for some time that successive methylation of pentafluorophosphorane produces a steady effect wherein the P-F axial bonds, $(P\text{-}F)_{ax}$, increase in length faster than do the remaining P-F equatorial bonds, $(P\text{-}F)_{eq}$. See Table I.

These phenomena have been discussed in terms of electron pair repulsion theory by Gillespie[7] and qualitative molecular orbital theory by Bartell[8] and Gavin.[9] The present work represents the results of a series of extended Hückel[10] and CNDO/2[11] calculations wherein the structures $PF_5$, $PF_4CH_3$, $PF_3(CH_3)_2$, $PF_2(CH_3)_3$, $PF_4H$, $PF_3H_2$, and $PF_2H_3$ were examined and some optimization performed using CNDO/2 calculations.

## Results and Discussion

Ideally the effect of substitution on bond length could be investigated through bond length optimization. However, the extended Hückel method does not generally yield satisfactory bond lengths upon optimization and our approach instead is to use Mulliken overlap populations as indicators of bond strength (and thus length) while actually holding the bond length constant for the various calculations.

We start by examining the effect of equatorial group electronegativity as shown in Figure 1 where we show the effect of successive methylation and hydrogenation in the equatorial positions of a $PF_5$.[12] The overlap populations show that the axial P-F bonds are weakened much more by substitution than are the remaining P-F equatorial bonds. Furthermore, it is interesting that the effect is approximately linear with the extent of substitution.

We may now inquire as to the source of the $(P\text{-}F)_{ax}$ overlap population decrease relative to the remaining $(P\text{-}F)_{eq}$ overlap populations. More specifically, we ask if the decrease is localized in the $\sigma$ or $\pi$ type interactions of the $(P\text{-}F)_{ax}$ bond. Furthermore, what is the role of d orbitals.

We start our inquiry by examining a model compound, $PL_2L_3^*$, wherein both L and L* resemble hydrogen atoms in that they bear only 1s orbitals and both the P-L and P-L* bond lengths are 1.44 Å. The L atoms occupy the axial positions and the L* the equatorial. Figure 2 shows the behavior of the $(P\text{-}L)_{ax}$ overlap population, a pure $\sigma$ interaction, as a function of the decreasing electronegativity (i.e., the value of $H_{ii}$) of the equatorial L* atoms. (The value of $H_{ii}$ for L is kept at $-18.0$ eV.) Without utilizing d orbitals there is a progressive decrease in the total overlap population for the $(P\text{-}L)_{ax}$ bond. Examining the contributions from the individual molecular orbitals shows that the weakening originates in the $2a_1'$ orbital. In order to understand this behavior we employ the interaction diagrams of Figure 3. In the middle of the diagram are the localized $\sigma$ and $\sigma^*$ $(P\text{-}L)_{ax}$ combinations, which are not affected (in the Hückel approximation) by the changes in the electronegativity of the equatorial L* atoms. When the L* atoms are of high electronegativity (left side of Figure 3) the $2a_1'$ orbital is derived primarily from the mixing of the $L_3^*$ fragment and the axial $\sigma$ combination. There is not much incorporation of the axial $\sigma^*$ fragment. On the other hand, when the $L_3^*$ is of higher energy (right side of Figure 3), both the axial $\sigma$ and $\sigma^*$ combinations mix into the $2a_1'$ orbital. Since the axial $\sigma$ fragment is lower lying, it mixes in $(P\text{-}L)_{eq}$ antibonding while the higher lying $\sigma^*$ combination mixes in bonding. There is a cancellation occurring in the contribution from the 3s orbital of the P and the $2a_1$ orbital is essentially nonbonding. Now, as the electronegativity of the L* atoms is decreased the energy of the $L_3^*$ fragment is increased (as shown on the right of Figure 3). The energy gap between the $\sigma^*$ combination and the $L_3$ fragment is lessened and the mixing of the $(P\text{-}L)_{ax}$ $\sigma^*$ fragment into the $2a_1$ orbital increased. As a result the $2a_1'$ orbital becomes more decidedly $(P\text{-}L)_{ax}$ antibonding. On the other hand, the lowest occupied valence shell orbital, $1a_1'$, will have a more bonding $(P\text{-}L)_{ax}$ interaction as the L* electronegativity increases. This is simply because the $1a_1'$ orbital will become more and more the pure $(P\text{-}L)_{ax}$ $\sigma$ combination of Figure 3.

Turning to the "with d" results displayed in Figure 2 we